Regeneration and Enhanced Catalytic Activity of Pt/C Electrocatalysts

Mingbo Ruan,[†] Xiujuan Sun,[†,‡] Yuwei Zhang,[†] and Weilin Xu*,[†]

[†]State Key Laboratory of Electroanalytical Chemistry, Changchun Institute of Applied Chemistry, Jilin Province Key Laboratory of Low Carbon Chemical Power, Chinese Academy of Science, 5625 Renmin Street, Changchun 130022, People's Republic of China

[‡]Graduate University of Chinese Academy of Science, Beijing, 100049, China

S *Supporting Information*

ABSTRACT: By adding pure carbon support to improve the redispersion of platinum (Pt), a sintered Pt/C electrocatalyst for methanol electrooxidation was effectively regenerated in activity and doubled in amount on the basis of a one-step liquid oxychlorination. The apparent activity (mA $mg_{cata.}^{-1}$) of the optimal Pt/C regenerated (Pt 3.3 wt %) is close to the initial fresh Pt/C (Pt 10 wt %) and about two times that of fresh Pt/C (Pt 3.3 wt %), making Pt utilization doubled and then the resource-limited Pt potentially sustainable. The new nucleation of metal atoms on added pure support surface was found to be the key for both the improved redispersion of metal nanoparticles and the effective regeneration of catalytic activity in situ.

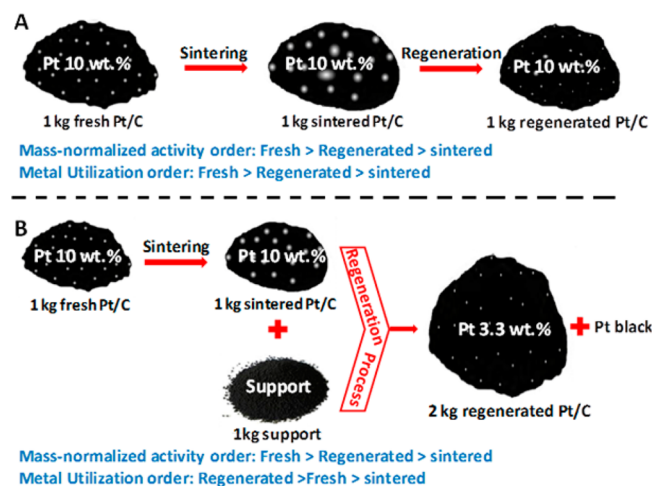**KEYWORDS:** *regeneration, precious metal, electrocatalyst, Pt, support*
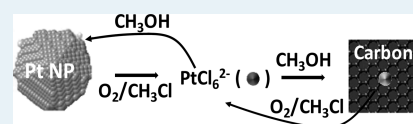
1. INTRODUCTION

Because of the limited resources of precious metals, regeneration of supported precious metal catalysts through the redispersion of metals is a highly interesting and significant topic, in particular because it is the reverse of deactivation, mainly as a result of the sintering.[1−3] Metal redispersion is a complex physical and chemical process that is dependent on temperature, atmosphere, time, and support.[4] It is also strongly influenced by the metal and its loading or promoters as well as by catalyst preparation. Redispersion has been applied successfully for many different supported metals, such as Pt,[2,5] Pd,[6−8] Au,[1,4] Rh,[9] Co,[10] Ni,[11] and Ag.[12] All these cases of redispersion, however, are based on only a simple reforming process of the original amount of metals on the original amount of supports, without a decrease in the metal loading or increase in the metal utilization, just like that shown in Scheme 1A.[4,5] All these previous results clearly show that the simple reformation or redispersion of precious metals on the original amount of support is effective, but not enough for the final practical application of precious metals because the utilization of precious metals did not increase.[13]

Herein, we present a simple one-step strategy to regenerate the catalytic activity and double the amount of carbon-supported platinum (Pt/C) electrocatalysts for methanol electrooxidation by adding carbon support only (Scheme 1B). A new surface on an additional carbon support can tremendously improve the redispersion of metal on the basis of new nucleation of the metal on the added new support surface. The mass-normalized catalytic activity (mA/mg of catalyst) of the optimal regenerated Pt/C (Pt 3.3 wt %) is two times the fresh Pt/C, with Pt 3.3 wt %, and close to that of the original fresh Pt/C (Pt 10 wt %). The Pt utilization of the optimal Pt/C regenerated is 250% that of the fresh catalyst. With this method, one can potentially obtain sustainable high

Scheme 1. The Mechanism for the Traditional Regeneration Process of Sintered Catalysts and the Regeneration Mechanism Based on the Addition of Pure Support[a]

[a](A) The utilization of precious metal on regenerated catalyst is lower than that of fresh one due to the incomplete activity regeneration and the same precious metal loading. (B) The utilization of precious metal on regenerated catalyst is higher than the fresh one as a result of much lower precious metal loading and doubled amount.

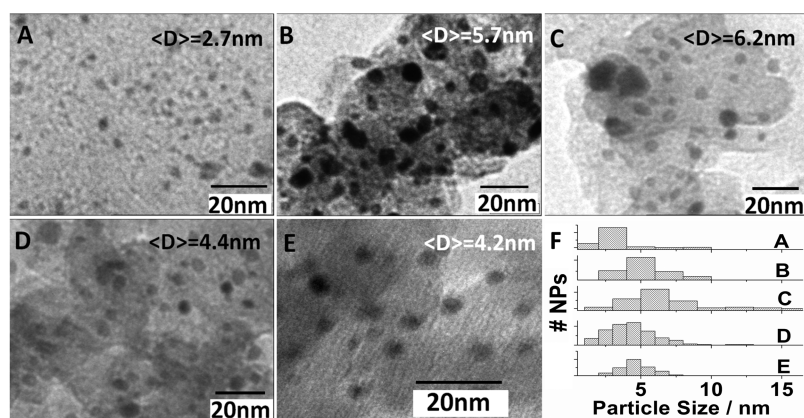performance Pt/C electrocatalysts based on the recycling of limited resource of Pt.

Figure 1. TEM characterization of different Pt/C catalysts: (A) fresh Pt/C (**Pt10**), (B) sintered Pt/C (**Pt-S**) at 900 °C under nitrogen atmosphere, (C) Pt/C obtained after the reforming of **Pt-S** in CH_3OH and CH_3Cl without additional carbon (**Pt-S-nc**), (D) Pt/C obtained after the reforming of **Pt-S** in CH_3OH and CH_3Cl with 6 mg additional Vulcan XC-72 carbon black (**PtS-6**), and (E) Pt/C obtained after the reforming of **Pt-S** in CH_3OH and CH_3Cl with 6 mg of additional BP carbon black (**PtS-BP**). (F) The histograms of Pt nanoparticle size distributions of above different Pt/C.

2. EXPERIMENTAL SECTION

2.1. Materials. Carbon black BP2000 was purchased from Asian-Pacific Specialty Chemicals, Kuala Lumpur; Vulcan XC-72 was purchased from E-TEK Com. Methanol (CH_3OH), sulfric acid (H_2SO_4), Nafion solution (5 wt %), and H_2PtCl_6·$6H_2O$ salt were purchased from Sigma-Aldrich. All the chemicals were used as delivered without further treatment. Ultrapure water with a specific resistance of 18.23 MΩ·cm was obtained by reversed osmosis, followed by ion exchange and filtration. A glassy carbon electrode (4 mm in diameter) was purchased from Tianjin Aida Hengsheng Tech. Co., China. High-purity CO (99.99%) was purchased from Changchun Gas Co., China.

2.2. Synthesis of Fresh Pt/C Electrocatalyst with Different Pt Loadings and Their Sintering. Vulcan XC-72 and H_2PtCl_6 were used as the carbon support and platinum precursor, respectively. The carbon support (1.0 g) was dispersed with known amounts of Pt precursor in 100 mL of deionized water and 50 mL of ethylene glycol, followed by sonication of ∼30 min for even dispersion. After that, a solution prepared by mixing ethylene glycol with sodium borohydride (molar ratio of ethylene glycol/$NaBH_4$ = 10:1) was added slowly drop-by-drop into the above solution with vigorous stirring. The mixture was kept stirring for 4 h at 100 °C to permit the complete reduction of Pt from its metal salt. The black precipitate was isolated on a filter, washed with deionized water, and then dried at 120 °C overnight to give a carbon-supported Pt catalyst. The Pt content was finally determined by ICP to be 10 wt % Pt. The prepared Pt/C catalyst was put in a quartz crucible, which was heated in N_2 atmosphere (flow rate: 200 mL/min) within a tubular furnace, and the temperature was increased to the set temperature (900 °C) with a ramp rate of 5 °C min^{-1}, followed by a dwell time at this temperature for 3 h. The sintered Pt/C with Pt 10 wt % was labeled as **Pt-S**.

2. 3. The Regeneration of Sintered Pt/C. The regeneration of sintered Pt/C was based on the fact that O_2/CH_3Cl can dissolve Pt nanoparticles into $PtCl_6^{2-}$ in a sealed refluxing methanol liquid environment, and the $PtCl_6^{2-}$ can be reduced back into Pt^0 by methanol when the temperature rises up to 160 °C. By combining these two processes together, we designed a redispersion or regeneration reaction system containing O_2, CH_3Cl, and methanol plus Pt/C in a sealed glass reactor from SynthWare. According to parameters from the manufacturer, the glassware shown in Figure S1 (Supporting Information) can stand high pressure up to 8 bar with a thick wall.

2. 4. Physical and Electrochemical Characterization of Catalysts. The morphology and dimensions of the as-prepared samples were obtained using transmission electron microscopy (TEM) obtained on a JEM-2100F microscope with an accelerating voltage of 200 kV. The Brunauer−Emmett−Teller (BET) surface areas and pore volumes were obtained from 77 K N_2 sorption isotherms using an ASAP 2020 instrument. X-ray photoelectron spectroscopic (XPS) measurements were performed on an AXIS Ultra DLD (Kratos company) using a monochromic Al X-ray source and carbon as the reference for binding energy. The powder X-ray diffraction (XRD) patterns were recorded on a Shimadzu XRD-6000 diffractometer with Cu K radiation. The final Pt contents in the catalysts were obtained from ICP (ICAP-6000, Thermo Fisher Scientific). The activity of Pt/C for methanol electrooxidation was evaluated by cyclic voltammetry (CV) on glassy carbon electrodes.

Fabrication of the working electrodes was done by pasting catalyst inks on a glassy carbon rotating disk electrode (4 mm in diameter). Its apparent surface area (0.1256 cm^2) was used to normalize the ORR activity of the catalysts. The carbon ink was formed by mixing 5 mg of Pt/C catalysts, 100 μL of 5 wt % Nafion solution in alcohol, and 900 μL of ethanol in a plastic vial under ultrasonication. A 10 μL aliquot of the carbon ink was dropped on the surface of the glassy carbon rotating disk electrode, yielding an approximate catalyst loading of 0.05 mg. The electrolyte was 0.5 M H_2SO_4 or 0.5 M H_2SO_4 + 0.5 M CH_3OH solution; the counter and reference electrodes were a platinum wire and a SCE electrode, respectively. The potential of the electrode was controlled by an EG&G (model 273) potentiostat/galvanostat system. Cyclic voltammetry was performed from 0.0 to 1.0 V at 50 mV s^{-1}. The electrochemically active surface areas (EASAs) were obtained through both a CO stripping method and H-upd (underpotentially deposited hydrogen) analysis.[14]
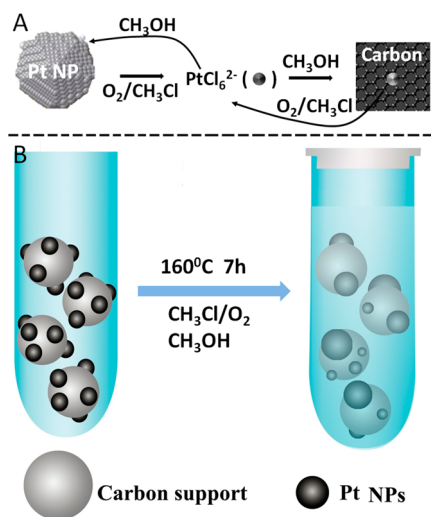
3. RESULTS AND DISCUSSION

In this work, the fresh Pt/C (2.4, 3.3, 4.4, and 10 wt % of Pt, labeled as **Pt2.4**, **Pt3.3**, **Pt4.4**, and **Pt10**) catalysts were prepared according to literature.[15] The obtained Pt nano-

particles on **Pt10** possess an averaged diameter of ∼2.7 nm (Figure 1A). The fresh **Pt10** was then sintered at 900 °C under N_2 flow for 3 h to obtain larger Pt nanoparticles with an average size of ∼5.7 nm (labeled as **Pt-S**, Figure 1B).

For the regeneration of **Pt-S** (Figure S1, Supporting Information), initially, we observed that the freshly obtained colloid Pt nanoparticles from the reduction of H_2PtCl_6 could be redissolved into $PtCl_6^{2-}$ when the colloid solution is boiled. The observed redissolving of colloid Pt nanoparticles was found to be actually an oxychlorination process in liquid phase.[5] On the basis of this phenomenon, we finally found out that oxygen/methyl chloride (CH_3Cl) in a sealed methanol-refluxing atmosphere can dissolve Pt nanoparticles into $PtCl_6^{2-}$ (Figure S2, Supporting Information), which could be reduced back to Pt^0 inversely by methanol when the temperature rises to 160 °C, just like that shown in Scheme 2. The obtained Pt^0 will deposit on either some extant Pt

Scheme 2. Redispersion Process of Pt on a Carbon Support[a]

[a](A) The molecular redox mechanism and equilibrium between Pt^0 and $PtCl_6^{2-}$, or balance between the deposition of Pt on extant Pt nanoparticles and the deposition of Pt^0 on carbon support. The oxidation of Pt^0 into $PtCl_6^{2-}$ was caused by O_2/CH_3Cl; the reduction of $PtCl_6^{2-}$ into Pt^0 was caused by methanol. (B) The scheme for the simple reforming of Pt on the original carbon support, which leads to a further size increase of the Pt nanoparticles.

nanoparticles or on a carbon surface as nuclei for the growth of new Pt nanoparticles. The reversible redox process of Pt proceeds simultaneously in a repeated manner for many cycles until a new equilibrium state is established (Scheme 2A) with the consumption of O_2/CH_3Cl and methanol. In this way, the majority of Pt nanoparticles will be reformed or redispersed onto a support as new Pt nanoparticles; the remaining Pt will stay in solution as $PtCl_6^{2-}$, which can be collected from the supernatant after centrifugation and then recovered in the form of black Pt powder with a strong reductant (Scheme 3). For the reforming of sintered Pt nanoparticles without any additional carbon support, as shown in Scheme 2B, the reduced Pt atoms tend to deposit on extant Pt nanoparticles rather than forming new nuclei on a carbon support, which makes the large nanoparticles larger and small nanoparticles smaller, just like that shown in the histograms of size distribution in Figure 1F, and finally, the average size of Pt nanoparticles obtained increases a little bit from 5.7 to 6.2 nm, as shown in Figure

1C,F (noted as **Pt-S-nc**), probably following the mechanism of seeded growth.[16,17]

The catalytic activities of these Pt/C catalysts were characterized on the basis of electrooxidation of methanol in an acid condition (Figure S3, Supporting Information). From the CV results shown in Figure 2A, we can see the fresh **Pt10** shows very high mass-normalized activity, with a peak current of 14 mA/mg catalyst in the positive scan direction. After sintering at 900 °C, the Pt/C was deactivated painstakingly, and only one-third of the original activity was maintained with a small peak current of ∼5 mA/mg catalyst (**Pt-S**). Obviously this deactivation is due mainly to the aggregation of Pt nanoparticles (Figure 1B) during the sintering process,[1] which also leads to the decrease in Pt utilization, as shown in Figure 2B. For the regeneration or redispersion of **Pt-S** using the protocol shown in Scheme 2B, without additional new support of carbon, the obtained **Pt-S-nc** shows the lowest activity for methanol electrooxidation, as shown in Figure 2A, as a result of the lower Pt loading (6 wt %) and the further increased size of the Pt nanoparticles, as shown in Figure 1C.

For the reduction of dissolved $PtCl_6^{2-}$ by methanol, as shown in Scheme 2A, there is a competition or balance between the nucleation on the carbon support and the deposition on extant Pt nanoparticles. Generally, the metal atoms prefer to deposit on extant same type of metal nanoparticles.[16] To improve the redispersion of the metal atoms, one would like to drive the balance to the right side and form more new nuclei or seeds on the support surface, as shown in Scheme 2A.

For that goal, we tried adding some pure support (carbon black) to the redispersion system. The addition of pure support is expected to dilute the concentration of Pt nanoparticles and drive the balance to the right side of Scheme 2A. It will lead to the nucleation of Pt^0 on a new carbon support for the growth of new Pt nanoparticles, as shown in Scheme 4, and finally lead to an improved redispersion or regeneration. First, it was found that a new equilibrium state, shown in Scheme 2A, could be established with the redispersion of the majority (67%) of Pt as nanoparticles after a long reaction time (>6 h) for a system of 6 mg of Vulcan XC-72 + 6 mg of sintered Pt/C (**Pt-S**) (Figure S4, Supporting Information). Furthermore, with a fixed reaction time of 7 h, 3 and 9 mg of pure Vulcan XC-72 were added to 6 mg **Pt-S**, respectively. Interestingly, as shown in Figure 2A, after the addition of the 3 and 6 mg of Vulcan XC-72 carbon, the final Pt loadings were decreased from 10 wt % to 4.4 and 3.3 wt % tested from ICP, respectively, but the mass-normalized activities (7 and 8 mA/mg catalyst) of the final catalysts (noted as **PtS-3** and **PtS-6**) all exceed that of **Pt-S**. Even for the one with an additional 9 mg of Vulcan XC-72 (**PtS-9**) with Pt loading of 2.4 wt %, the final mass-normalized activity is much higher than the fresh Pt/C with Pt 2.4 wt % (Figure S5, Supporting Information). Among these three, the **PtS-6** shows the best performance, with a 50% increase in the mass-normalized activity and 70% decrease in the Pt consumption compared with **Pt-S**. Obviously the addition of pure carbon support to the reaction system is indeed an effective way to drive the balance to the right side of Scheme 2A and finally form more new nuclei or growth centers on support. The new seeds or growth centers on the new support greatly enhance the redispersion of Pt, as indicated from the smaller size of the Pt nanoparticles (≈4.4 nm in diameter) for the **PtS-6** (Figure 1D), which is consistent with the expectation. The best performance of **PtS-6** among these three regenerated
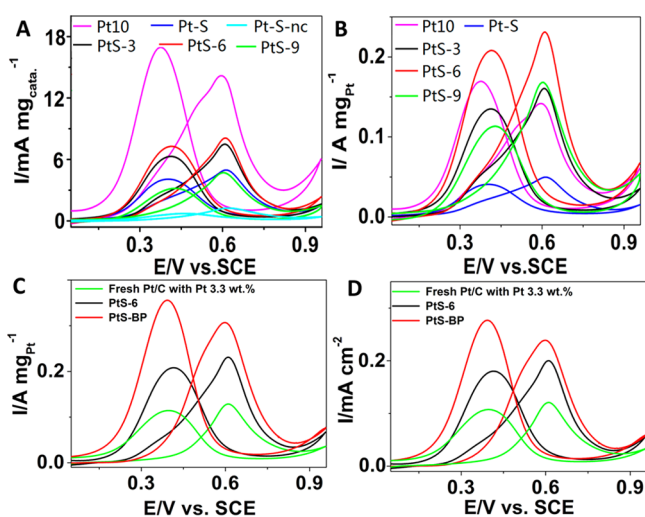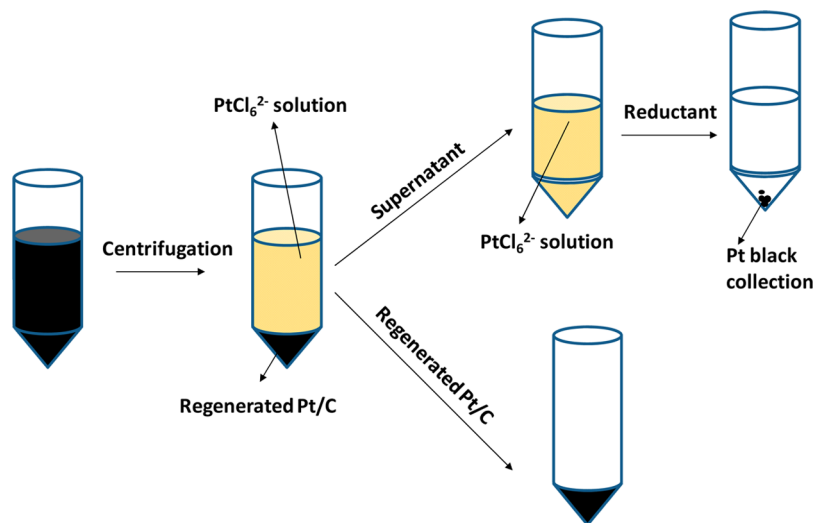
Scheme 3. Recovery of Pt from PtCl$_6^{2-}$ after the Regeneration Process of Pt/C

Figure 2. Electrocatalytical characterization of different Pt/C catalysts through CV in 0.5 M H$_2$SO$_4$ and 0.5 M CH$_3$OH solution with scan rates of 50 mV/s. (A) Comparison of catalyst mass-normalized catalytic activity (mA/mg catalyst) among different catalysts: fresh Pt/C (**Pt10**), sintered **Pt-S**, reformed one (**Pt-S-nc**) without addition carbon based on **Pt-S**, reformed ones (**PtS-3**, **PtS-6**, **PtS-9**) with addition of different amounts (3, 6, and 9 mg) of Vulcan XC-72 based on **Pt-S**. (B) Comparison of Pt mass-normalized catalytic activity (A mg$_{Pt}^{-1}$) among different catalysts: fresh Pt/C (**Pt10**), sintered **Pt-S**, reformed **PtS-3**, **PtS-6**, and **PtS-9** based on **Pt-S**. (C) Pt utilization (A mg$_{Pt}^{-1}$) comparison among fresh Pt/C, **PtS-6**, and **PtS-BP**. These three catalysts have the same Pt content of 3.3 wt %. (D) Pt utilization (mA cm^{-2}) comparison among fresh Pt/C, **PtS-6**, and **PtS-BP**. These three catalysts have the same Pt content of 3.3 wt %. The area used is the EASA obtained from the CO stripping method.

ones indicates there is an optimal amount of added carbon support, which can lead to the best performance of regenerated catalysts.

More interestingly, as shown in Figure 2B, the mass-normalized activity per milligram of Pt (A mg$_{Pt}^{-1}$) for the catalysts with additional pure carbon support are all more than 3 times higher than that of sintered Pt/C, indicating greatly improved utilization of Pt as a result of the successful redispersion of Pt on carbon. More significantly, the Pt utilizations (A mg$_{Pt}^{-1}$) of the regenerated catalysts with 3 and 9

Scheme 4. Improved Redispersion/Regeneration of Pt Nanoparticles Based on Additional Support[a]
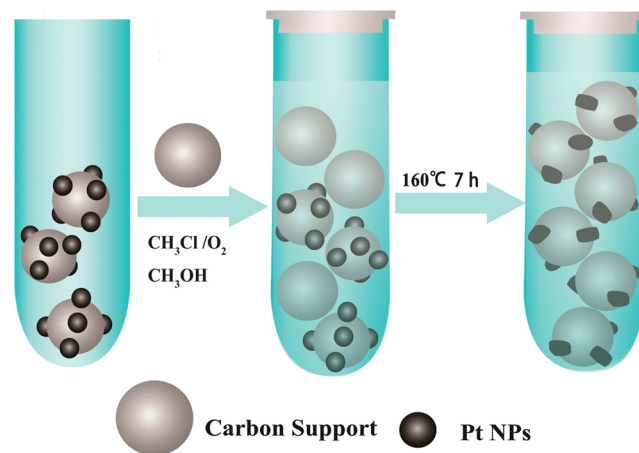
[a]Additional pure carbon support was added into the reaction system to dilute the Pt nanoparticle concentration and supply a clean surface for the nucleation of Pt atoms and potentially improve the redispersion of metal nanoparticles.

mg of Vulcan XC-72 also reach the level of fresh Pt/C; the one with an additional 6 mg of Vulcan XC-72 even shows a 40% higher Pt utilization than that of fresh **Pt10**.

To further evaluate the Pt utilization of optimal regenerated Pt/C catalysts, a series of fresh Pt/C with different Pt contents (2.4, 3.3, 4.4 wt %) were prepared using the same protocol as that for **Pt10**. The electrochemical active surface area obtained from CO-stripping (EASA$_{CO}$) of the samples was obtained and correlated with the activity results.[18] As an example shown in Figure 2C,D, the Pt utilization (A mg$_{Pt}^{-1}$ or mA cm^{-2} of EASA$_{CO}$) of the best regenerated **PtS-6** is ∼70% higher than that of fresh Pt/C with the same Pt content of 3.3 wt % . Although the obtained catalyst **PtS-6** shows higher Pt utilization, its apparent activity (mA/mg catalyst), which is one of the most important and practical parameters for the evaluation of a catalyst, shown in Figure 2A is still lower than the initial fresh **Pt10**.

That means that to get some practical regenerated catalysts based on sintered deactivated ones, we need to further improve

the dispersion of reformed metal nanoparticles on an added new support during the reforming process of precious metals. For that goal, we tried another type of inexpensive carbon black: Black Pearls 2000 (BP). It possesses much larger (Brunauer−Emmett−Teller) BET surface area (1391 m^2/g) than Vulcan XC-72(235 m^2/g).[19] It is expected that the larger surface will supply more potential active sites for the deposition of Pt^0 and then minimize its self-deposition on extant Pt nanoparticles and drive the balance in Scheme 2A farther to the right.[20,21] Indeed, interestingly, for the addition of 6 mg of pure BP to the 6 mg **Pt-S**, the obtained catalyst (**PtS-BP**) shows a smaller average size of ∼4.2 nm (Figure 1E) and a higher mass activity (11 mA/mg catalyst in Figure 3A) compared with **PtS-**

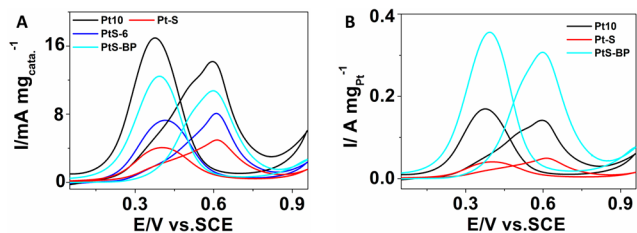**Figure 3.** Electrocatalytical characterization of different Pt/C catalysts through CV in 0.5 M H_2SO_4 and 0.5 M CH_3OH solution with scan rates of 50 mV/s. (A) The comparison of mass-normalized catalytic activity (mA/mg catalyst) among different catalysts: fresh Pt/C (**Pt10**), sintered **Pt-S**, reformed **PtS-6**, reformed one (**PtS-BP**) with addition of 6 mg BP based on **Pt-S**. (B) The comparison of Pt mass-normalized catalytic activity (A/mg Pt) among different catalysts: fresh Pt/C (**Pt10**), **Pt-S**, **PtS-BP**.

6 based on the addition of 6 mg of Vulcan XC-72. These data unambiguously further confirm the above expectation or the mechanism shown in Scheme 2A. Compared with **PtS-6**, the higher mass-normalized activity of 11 mA/mg catalyst with Pt 3.3 wt % is more practical and closer to the 14 mA/mg catalyst of fresh **Pt10**. The Pt utilization of **PtS-BP** is more than 2 times that of the fresh **Pt10** (Figure 3B) and 2.5 times that of fresh Pt/C with the same Pt 3.3 wt % (Figure 2C,D).

To further confirm that the above strategy or mechanism shown in Scheme 4 is also applicable to other sintered Pt/C catalysts, we studied the regeneration of sintered Pt/C with Pt 4.4 wt %. Interestingly, as shown in Figure S6 (Supporting Information), by adding pure carbon support, the Pt utilizations of the regenerated catalysts are higher than that of the fresh one (**Pt4.4**), further confirming the feasibility of the strategy proposed in Scheme 4.

Obviously, the larger BET surface area of the added support with an appropriate amount allows the better redispersion of Pt and the better regeneration of catalytic activity. In principle, according to the mechanism shown in Scheme 2A, on the basis of added special supports with large BET surface areas to improve the redispersion of precious metals, it is possible to get regenerated catalysts with mass-normalized activity (such as mA/mg catalyst) as high as the fresh one and doubled amount, just like that shown in Scheme 1B. That means through this general method, we can hugely reduce the consumption rate of Pt or other precious metals but without much sacrifice of mass activity of catalysts by simply adding an inexpensive support to double or triple the amount of catalysts. Before this work, many research groups have reported the regeneration of sintered catalyst, but none of them can increase the utilization of precious metals with no additional support. So the work presented here is one of the most promising and practical strategies to relieve the resource crisis of precious metals.

Intrinsically, all the above regeneration of Pt/C is a redispersion process of making big Pt nanoparticles small, so is this "regeneration" or "redispersion" method also applicable for smaller size Pt nanoparticles? Or what if the fresh Pt/C rather than the sintered one is used as the Pt source? To answer those questions, the fresh Pt/C (**Pt10**) was "regenerated" in a way similar to the above with additional carbon. Interestingly, as an example shown in Figure 4, with the addition of 6 mg of Vulcan XC-72 carbon to 6 mg of **Pt10**, the obtained "regenerated" catalyst (**Pt10-6**) shows a decreased apparent activity (Figure 4A, mA mg_{cata}^{-1}) and no increase in Pt utilization (Figure 4B, A mg_{Pt}^{-1}) compared with **Pt10**. Obviously, one reason is the Pt loss; the other is the size increase (from 2.7 to 4.0 nm) of the reformed Pt nanoparticles, as shown in Figure 4C. Compared with the size decrease observed (from **Pt-S** to **PtS-6**) shown above in Figure 1, the size increase observed here for **Pt10-6** indicates that the "regeneration process" is only practically applicable to Pt/C with big (or sintered) Pt nanoparticles. If Pt nanoparticles on the Pt source (such as fresh Pt/C) are already very small, it would be much harder to make the size smaller compared with larger size Pt nanoparticles.

To chemically understand why the regeneration process is effective for sintered Pt/C, XPS was used to characterize the chemical nature of catalysts before and after the regeneration (Figure S7, Supporting Information). As shown in Table 1 for Pt 4f, compared with the Pt/C before regeneration (**Pt-S**), the content of the Pt^{2+} (oxide form) did not change much after the regeneration with either Vulcan XC-72 or BP as an additional
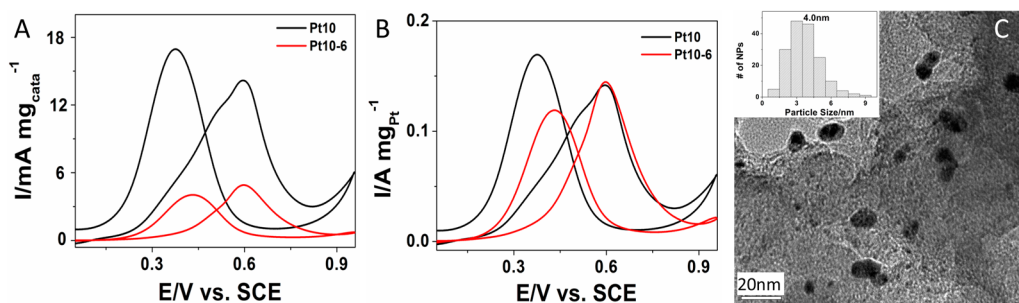

Figure 4. Effect of the "regeneration process" with additional carbon on the fresh Pt/C (**Pt10**): (A) decrease in the apparent activity (mA mg_{cata}^{-1}) after the treatment; (B) there is no improvement of Pt utilization (A mg_{Pt}^{-1}) after the regeneration process; (C) typical TEM image and the size distribution of Pt after the regeneration process.

Table 1. Summary of Pt 4f XPS Data for Different Pt/C Catalysts

Pt 4f	Pt10	Pt-S	PtS-6	PtS-BP
Pt^0 B.E. (content, %)	71.5 eV (68.7%)	70.3 eV (67.9%)	70.8 eV (72.9%)	71.2 eV (65.3%)
Pt^2 B.E. (content, %)	72.4 eV (31.3%)	71.2 eV (32.1%)	71.8 eV (27.1%)	72.0 eV (34.7%)

Table 2. Summary of C 1s XPS Data for Different Pt/C Catalysts

C 1s	C−C	C−O	O−C=O
Pt10 B.E. (content, %)	284.7 eV (84.4%)	286.6 eV (7.8%)	289 eV (7.8%)
Pt-S B.E. (content, %)	284.6 eV (76.9%)	286 eV (9.3%)	288.5 eV (13.8%)
Pt-S-nc B.E. (content, %)	284.5 eV (78.1%)	286 eV (9.1°%)	288.4 eV (12.8%)
PtS-BP B.E. (content, %)	284.8 eV (88.9%)	286.4 eV (3.3%)	288.8 eV (7.8%)

pure carbon support, indicating the catalytic activity of Pt/C catalysts is not directly related to the contents of the different chemical states of Pt,[22] although after the regeneration process, the binding energy of Pt (both Pt^0 and Pt^{2+}) shifted close to that of fresh Pt/C (**Pt10**) with either Vulcan XC-72 or BP as the additional carbon, and the BP led to a larger shift than Vulcan XC-72. The order of binding energy for these catalysts is the following: **Pt10 > PtS-BP > PtS-6 > Pt-S**. Interestingly, this order is coincidently the same as the apparent activities of these catalysts shown in Figure 2. Actually it has been well-known that the positive shifts of binding energy of Pt could lead to improved performance or activity of catalysts,[23,24] so this fact further explains the high performance of the regenerated catalysts compared with the sintered one.

Furthermore, the C 1s and O 1s XPS spectra for these catalysts can also reveal some information about the surface change of carbon during the redispersion process. As shown in Table 2 for the summary of C 1s, in the absence of additional carbon, from **Pt-S** to **Pt-S-nc**, neither the contents nor the binding energy of the carbon species (C−C, C−O and O−C=O) showed much change; whereas with additional carbon, such as from **Pt-S** to **PtS-BP**, the contents of carbon oxide species (C−O and C=O) decreased hugely, indicating much less −COO$^-$ on the carbon surface of **PtS-BP** compared with **Pt-S** or **Pt-S-nc**. More importantly, the binding energy of all the three carbon species positively shifted after the addition of carbon. Similar conclusions can be made from the O 1s XPS spectra summarized in Table 3. The observed chemical shifts of

Table 3. Summary of O 1s XPS Data for Different Pt/C Catalysts

O 1s	C=O	C−O
Pt10 B.E. (content, %)	532.3 eV (57.6%)	533.7 eV (42.6%)
Pt-S B.E. (content, %)	531.6 eV (57.7%)	533 eV (42.3%)
Pt-S-nc B.E. (content, %)	531.7 eV (52.9%)	533.1 eV (47.1%)
PtS-BP B.E. (content, %)	532 eV (50%)	533.4 eV (50%)

C 1s and O 1s to higher binding energy with additional carbon could be explained by a decrease in the electron charge density of the carbon or carbon oxide species due to a decrease in their electronic polarizability. Decreased polarizability means weaker electron donor ability of these species or weaker repelling to negatively charged PtCl$_6^{2-}$, making the adsorption of PtCl$_6^{2-}$ on carbon more easily compared with the carbon surface with the lower binding energy.[25] The easier adsorption of PtCl$_6^{2-}$ on carbon will make the Pt nucleation easier on pure carbon and then improve the redispersion of Pt by forming more new Pt NPs on the carbon surface.

In all these regenerated samples, as a result of the thorough water-washing, no chloride could be detected from either XPS or elementary analysis after the regeneration reaction, so the possible effect of chloride on the catalysts could be neglected. From the increase in the mass-normalized activity, we can deduce that the exposure of more active sites induced from the surface reconstruction probably is the main reason for the increase in the activity of these regenerated catalysts.

To further understand the correlation between the crystal structures and the catalytic activities of Pt nanoparticles on these catalysts, they were characterized with XRD spectra (Figure 5A). The intensity ratio between the (111) peak and (200) peaks ($I_{(111)}/I_{(200)}$) was used to quantify the variation of the Pt(111) facet on these catalysts after regeneration.[14] Interestingly, the results show the regeneration process can greatly increase this ratio, indicating the exposure of more (111) facets on the Pt nanoparticles after the regeneration process. More importantly, as shown in Figure 5B, the $I_{(111)}/I_{(200)}$ ratio is positively correlated with the Pt utilization of these catalysts (correlation coefficient: $R = 0.95$), unambiguously confirming the exposure of the (111) facet is one of the main reasons for the increase in the catalytic activity for methanol oxidation or the (111) facet is more active than the (200) facet for this catalytic reaction.[14]

To understand the structure−activity correlation of Pt/C catalysts from different perspectives, the correlation between the EASAs and the Pt utilizations was studied. The EASA for each catalyst was obtained in two different ways. As shown in Figure S8 (Supporting Information), one is from CO-stripping (EASA$_{CO}$),[14] and the other (EASA$_H$) is from the analysis of H-upd (underpotentially deposited hydrogen) on Pt/C surface.[14] The correlations of these two EASAs with Pt utilization (A mg$_{Pt}^{-1}$) were studied for 10 different Pt/C catalysts, as shown in Figure 6. Interestingly, both EASA$_{CO}$ and EASA$_H$ are positively correlated with Pt utilization of catalysts for methanol electrooxidation. These results indicate the following two important facts: (i) the regeneration process can greatly enhance the Pt utilization by exposing more catalytic active sites, which are mainly on the Pt (111) facet, according to XRD results shown in Figure 5; and (ii) the active sites on Pt/C catalysts for methanol electrooxidation are related to the adsorption sites of CO or H. That is why both EASA$_{CO}$ and EASA$_H$ could be used to characterize the electrocatalytic properties of catalysts by many other groups,[14] although EASA$_{CO}$ shows a stronger correlation (with correlation coefficient $R_{CO} = 0.88$) with Pt utilization than EASA$_H$ does ($R_H = 0.78$), indicating that the CO adsorption sites on Pt are more structurally similar to the active sites for methanol oxidation than H adsorption sites, probably due to the fact that
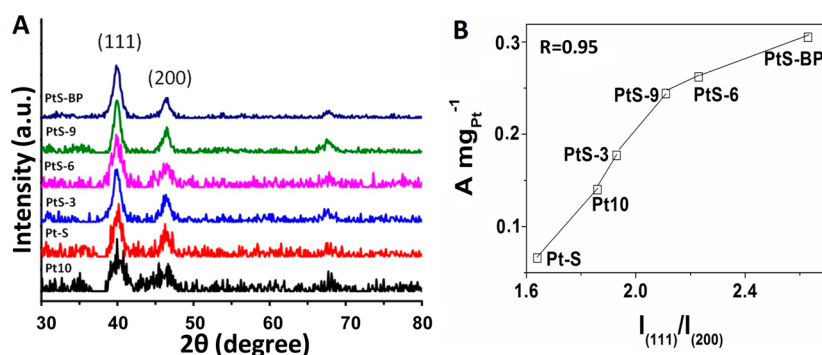
Figure 5. (A) XRD spectra of different Pt/C catalysts. (B) Correlation between $I_{(111)}/I_{(200)}$ and Pt utilization (A mg_{Pt}^{-1}) of different Pt/C catalysts.

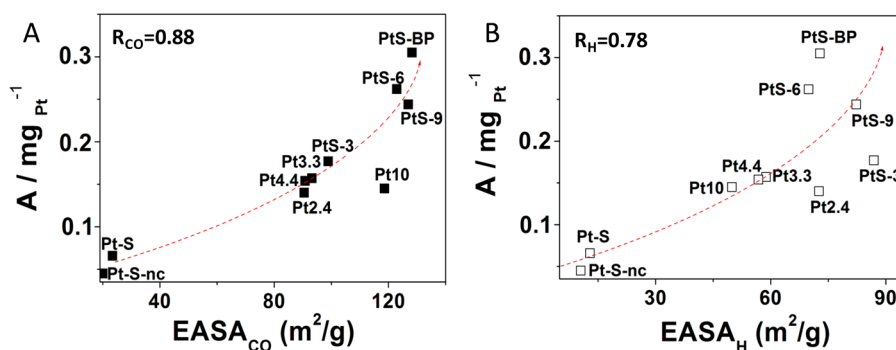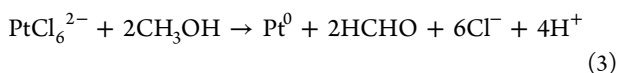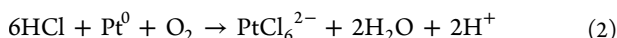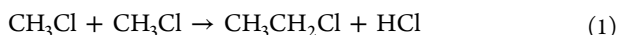**Figure 6.** Correlation between Pt utilization and $EASA_{CO}$ (A) or $EASA_H$ (B) for 10 different Pt/C catalysts. The red arrows show their positive dependences.

CO_{ad} is one of the intermediates for methanol electrooxidation on Pt.[26]

To further understand the molecular mechanism of the reversible redox or redispersion process of Pt in the liquid phase, the gas phase product from the treatment of Pt/C in *n*-hexane-mediated O_2/CH_3Cl liquid phase was analyzed with gas chromatography (GC, Figure S9, Supporting Information). Only one new species of CH_3CH_2Cl was detected. As for the reductant of methanol for the reduction of $PtCl_6^{2-}$, it was known the methanol was oxidized into methanal.[27] On the basis of these facts, we propose the following possible molecular mechanism for the Pt reforming process:

$$CH_3Cl + CH_3Cl \rightarrow CH_3CH_2Cl + HCl \qquad (1)$$

$$6HCl + Pt^0 + O_2 \rightarrow PtCl_6^{2-} + 2H_2O + 2H^+ \qquad (2)$$

$$PtCl_6^{2-} + 2CH_3OH \rightarrow Pt^0 + 2HCHO + 6Cl^- + 4H^+ \qquad (3)$$

From this mechanism, we can see the oxygen and chlorine are two important reagents for the whole redispersion process of Pt, which make the mechanism similar to the well-known oxychlorination.[5,28] The traditional oxychlorination process is a gas-phase reaction at high temperature (>600 °C) to redisperse metals in the oxidation state; it is followed necessarily by a reduction process of oxidized metal. That means the whole regeneration process needs to be done in two tandem steps in a flowing gas phase at high temperature, whereas in the case reported here, these two steps (oxidation and reduction) can be done in one step simply in a sealed liquid environment at much lower temperature. This is also the first case of using liquid oxychlorination to redisperse or regenerate catalyst. The refluxing liquid and low temperature environment make the

redispersion control of metal nanoparticles much easier and more environmentally friendly as a result of the much lower consumption of chemicals and energy.

4. CONCLUSION

In conclusion, by adding inexpensive carbon support to improve the redispersion of Pt, the sintered Pt/C electrocatalyst was effectively regenerated in activity for methanol electrooxidation with much lower Pt consumption. This general method makes Pt or other precious metals potentially sustainable based on the effective recycling of limited resource. A general mechanism for the improved redispersion and effective activity regeneration of catalysts was also presented. This work opens a new direction to sustainably get new functional high-performance materials from limited resources.

■ ASSOCIATED CONTENT

ⓢ Supporting Information

The following file is available free of charge on the ACS Publications website at DOI: 10.1021/cs5013427.

> Materials and methods; experimental details; control experiments (PDF)

■ AUTHOR INFORMATION

Corresponding Author
*Fax: +86-431-85262848. E-mail: weilinxu@ciac.ac.cn.
Notes
The authors declare no competing financial interest.

■ ACKNOWLEDGMENTS

2012CB215500), National Natural Science Foundation of China (21273220, 21303180), and "The Recruitment Program of Global youth Experts" of China.

■ REFERENCES

(1) Goguet, A.; Hardacre, C.; Harvey, I.; Narasimharao, K.; Saih, Y.; Sa, J. *J. Am. Chem. Soc.* **2009**, *131*, 6973−6975.

(2) Lee, T. J.; Kim, Y. G. *J. Catal.* **1984**, *90*, 279−291.

(3) Marinho, R. S.; Silva, C. N.; Afonso, J. C.; Cunha, J. W. S. D. *J. Haz. Mater.* **2011**, *192*, 1155−1160.

(4) Kartusch, C.; Krumeich, F.; Safonova, O.; Hartfelder, U.; Makosch, M.; Sa, J.; Bokhoven, J. A. *ACS Catal.* **2012**, *2*, 1394−1403.

(5) Galisteo, F. C.; Mariscal, R.; Granados, M. L.; Fierro, J. L. G.; Daley, R. A.; Anderson, J. A. *Appl. Catal. B: Environmental* **2005**, *59*, 227−233.

(6) Daley, R. A.; Christou, S. Y.; Efstathiou, A. M.; Anderson, J. A. *Appl. Catal., B* **2005**, *60*, 117−127.

(7) Newton, M. A.; Belver-Coldeira, C.; Martinez-Arias, A.; Fernandez-Garcia, M. *Nat. Mater.* **2007**, *6*, 528−532.

(8) Chen, J. J.; Ruckenstein, E. *J. Phys. Chem.* **1981**, *85*, 1606−1612.

(9) Van't Blik, H. F. J.; Van Zon, J. B. A. D.; Huizinga, T.; Vis, J. C.; Koningsberger, D. C.; Prins, R. *J. Am. Chem. Soc.* **1985**, *107*, 3139−3147.

(10) Chernavskii, P. A.; Pankina, G. V.; Zaikovskii, V. I.; Peskov, N. V.; Afanasiev, P. *J. Phys. Chem. C* **2008**, *112*, 9573−9578.

(11) Ruckenstein, E.; Lee, S. H. *J. Catal.* **1984**, *86*, 457−464.

(12) Shimizu, K.-i.; Katagiri, M.; Satokawa, S.; Satsuma, A. *Appl. Catal., B* **2011**, *108*, 39−46.

(13) Miyazaki, A.; Balint, I.; Nakano, Y. *J. Nanopart. Res.* **2003**, *5*, 69−80.

(14) Meher, S. K.; Rao, G. R. *ACS Catal.* **2012**, *2*, 2795−2809.

(15) Gharibi, H.; Kakaei, K.; Zhiani, M. *J. Phys. Chem. C* **2010**, *114*, 5233−5240.

(16) Wu, H. L.; Kuo, C. H.; Huang, M. H. *Langmuir* **2010**, *26*, 12307−12313.

(17) Yuan, L.; Yang, M.; Qu, F.; Shen, G.; Yu, R. *Electrochim. Acta* **2008**, *53*, 3559−3565.

(18) Kaiser, J.; Simonov, P. A.; Zaikovskii, V. I.; Hartnig, C.; Jörissen, L.; Savinova, E. R. *J. Appl. Electrochem.* **2007**, *37*, 1429−1434.

(19) Sun, X.; Song, P.; Zhang, Y.; Liu, C.; Xu, W.; Xing, W. *Sci. Rep.* **2013**, *3*, 2505−2509.

(20) Suttiponparnit, K.; Jiang, J.; Sahu, M.; Suvachittanont, S.; Charinpanitkul, T.; Biswas, P. *Nanoscale Res. Lett.* **2011**, *6*, 27−30.

(21) Wu, G.; Johnston, C. M.; Mack, N. H.; Artyushkova, K.; Ferrandon, M.; Nelson, M.; Lezama-Pacheco, J. S.; Conradson, S. D.; More, K. L.; Myers, D. J.; Zelenay, P. *J. Mater. Chem.* **2011**, *21*, 11392−11405.

(22) Koper, T. M. M. *Fuel Cell Catalysis: A Surface Science Approach.* Wiley: 2009.

(23) Shao, Y.; Sui, J.; Yin, G.; Gao, Y. *Appl. Catal., B* **2008**, *79*, 89−99.

(24) Wakisaka, M.; Mitsui, S.; Hirose, Y.; Kawashima, K.; Uchida, H.; Watanabe, M. *J. phys. Chem. B* **2006**, *110*, 23489−23496.

(25) Dimitrov, V.; Komatsu, T. *Phys. Chem. Glasses-B* **2003**, *44*, 357−364.

(26) Park, S.-H.; Joo, S.-J.; Kim, H.-S. *J. Electrochem. Soc.* **2014**, *161*, F405−F414.

(27) Teranishi, T.; Hosoe, M.; Tanaka, T.; Miyake, M. *J. Phys. Chem. B* **1999**, *103*, 3818−3827.

(28) Anderson, J. A.; Mordente, M. G. V.; Rochester, C. H. *J. Chem. Soc., Faraday Trans.* **1989**, *85*, 2983−2990.